

# Pesticide peak concentration reduction in a small vegetated treatment system controlled by chemograph shape

Jan Greiwe<sup>1</sup>, Oliver Olsson<sup>2</sup>, Klaus Kümmerer<sup>2</sup>, Jens Lange<sup>1</sup>

<sup>1</sup>Hydrology, University of Freiburg, Fahnbergplatz, 79098 Freiburg, Germany

<sup>2</sup>Institute of Sustainable and Environmental Chemistry, Leuphana University of Lüneburg, Scharnhorststr. 1, 21335 Lüneburg, Germany

*Correspondence to:* Jan Greiwe (jan.greiwe@hydrology.uni-freiburg.de)

**Abstract.** Pesticides may impact aquatic ecosystems when entering water bodies. Measures for mitigation against pesticide inputs include vegetated treatment systems (VTS). Some of these systems have very short hydraulic retention time ( $< 1$  h) but nevertheless manage to effectively reduce peak concentrations of contaminants as a result of dispersion. We hypothesize that the effect of dispersion on contaminant mitigation in VTS depends on the shape of the contaminant input signal chemograph which in turn is related to factors affecting contaminant mobilization in the contributing catchment. In order to test this hypothesis we grouped chemographs of 6 contaminants originating from a viticultural catchment during 10 discharge events into clusters according to chemograph shape. We then compared peak concentration reduction and mass removal in a downstream VTS both among clusters and in terms of compound properties and discharge dynamics. We found that chemograph clusters reflected combined effects of contaminant source areas, transport pathways, and discharge dynamics. While mass loss was subject to major uncertainties, peak concentration reduction rate was clearly related to chemograph clusters and dispersion sensitivity. These findings suggest that mitigation of acute toxicity in VTS is stronger for compounds with sharp-peaked chemographs whose formation is related to the contributing catchment and can be analyzed by chemograph clustering.

## 1 Introduction

Use of pesticides is beneficial for agricultural productivity. However, when pesticides reach surface water bodies, they threaten aquatic organisms (Zubrod et al., 2019). Effects of pesticides on aquatic ecosystems include a reduction of species richness of invertebrates (Beketov et al., 2013) as well as microorganisms (Fernández et al., 2015). Unintended export of pesticides from the application site to water bodies can happen in particulate form via erosion (Oliver et al., 2012; Taghavi et al., 2011) or in dissolved form via surface runoff, drainage pipes, spray drift or leakage to groundwater (Reichenberger et al., 2007) and subsequent exfiltration.

In the environment pesticides are subject to degradation by both abiotic (e.g. hydrolysis, photolysis) and biotic (e.g. plant metabolism, microbial degradation) processes (Fenner et al., 2013). If degradation is incomplete, pesticides form

transformation products (TPs) which in some cases may be equally or more mobile, persistent or toxic than their PCs (Hensen et al., 2020). Strongest mobilization of pesticides is usually associated with the first significant rainfall after application and fast discharge components (Doppler et al., 2012; Olsson et al., 2013; Lefrancq et al., 2017), e.g. runoff from non-target areas like roads (Lefrancq et al., 2013). Mobilization dynamics of TPs usually differ from those of their parent compounds (PCs) in terms of source areas and export pathways. The formation of TPs may happen on larger time scales and TPs usually have different physicochemical properties than their PCs (Gassmann et al., 2013). The specific transformation and further degradation of a contaminant largely depends on the interplay of the contaminant's mobility and degradability as well as site characteristics (Gassmann et al., 2015). Both mobility and degradability can vary over multiple orders of magnitude for different contaminants. However, water and soil half-lives are at least in the order of several days or weeks for most pesticides (Lewis et al., 2016).

Pesticide pollution can be mitigated by vegetated treatment systems (VTS) located between source areas and receiving water bodies (Vymazal and Březinová, 2015; Stehle et al., 2011; Gregoire et al., 2009). Such systems temporally retain polluted waters and thus provide space, time and favorable conditions for degradation processes. VTSs studied in literature include very different types of systems (Lange et al., 2011), including vegetated ditches or detention ponds with hydraulic residence times (HRT) ranging in the order of minutes to several hours (Bundschuh et al., 2016; Elsaesser et al., 2011; Ramos et al., 2019) or constructed wetlands in which HRT may reach several weeks (Maillard and Imfeld, 2014), particularly when operated in batch mode (Tournebize et al., 2017; Maillard et al., 2016; Moore et al., 2000). The term pesticide mitigation can refer to contaminant mass removal ( $R_M$ ) or peak concentration reduction ( $R_C$ ). While mass removal is mainly observed in systems with longer HRT and affects permanent toxicity, peak concentration reduction also happens in systems with short HRT where it reduces acute toxicity (Bundschuh et al., 2016; Elsaesser et al., 2011; Stehle et al., 2011).

During longitudinal transport in streams or wetlands, peak concentration reduction does not necessarily involve degradation but can solely be the result of enhanced dispersion due to the presence of obstacles such as plants (Elsaesser et al., 2011) and temporary removal from the water phase by reversible sorption. Mitigation properties therefore constantly change due to wetland succession (Schuetz et al., 2012). Regardless of whether VTSs target concentration reduction or mass removal, mitigation efficiency is usually associated with physicochemical properties of target compounds (Vymazal and Březinová, 2015) or VTSs, including their operation mode (Tournebize et al., 2017). However, following the concept of advective-dispersive transport (Fischer et al., 1979), the mitigating effect of dispersion on a concentration signal does not only depend on the magnitude of dispersion but also on the shape of the signal. Peak concentration reduction will be stronger for a signal with a pronounced peak and low background than for a signal with a small peak and high background if both signals are exposed to the same dispersion. Chemograph shapes, in turn, are dictated by processes in the contributing catchments. The influence of this chain of effects on contaminant mitigation and hence VTS efficiency has not been systematically investigated so far.

We hypothesize that the efficiency of contaminant mitigation in VTSs depends on the shape of the input chemographs and eventually on the factors that produce these signals in the catchment. In order to test this hypothesis we grouped chemographs

66 of 6 contaminants mobilized in a viticultural catchment during 10 discharge events into clusters according to chemograph  
67 shape. We then compared peak concentration reduction and mass removal in a downstream VTS both among clusters and in  
68 terms of compound properties and discharge dynamics.

## 69 **2 Material and methods**

### 70 **2.1 Study site**

71 The study site (Figure 1) is located inside a flood detention basin in the 1.8 km<sup>2</sup> Loechernbach catchment, southwest Germany.  
72 Catchment elevation ranges between 213 m.a.s.l. at the outlet and 378 m.a.s.l. in the western corner. Mean precipitation was  
73 800 mm a<sup>-1</sup> between 2009 and 2018, mean air temperature 11.3 °C. Soils mainly consist of calcaric regosols which formed on  
74 aeolian loess and have a typical grain size distribution of 10 % sand, 80 % silt and 10 % clay. Most of the catchment is  
75 dedicated to large artificial vineyard terraces (71 %), while croplands occupy the valley bottoms (20 %). Forest only accounts  
76 for a small portion (9 %) and is limited to the most elevated part of the catchment. This partition in land use is reflected in the  
77 main application areas of pesticide types. Fungicides are applied on vineyard terraces, while herbicides are mainly applied to  
78 the cropland in the flat valleys. Large parts of the catchment are drained by a sub-surface pipe network (Figure 1) connecting  
79 vineyards and paved roads to the main channel in the valley. This drainage network causes fast downstream transport of storm  
80 water and suspended sediments (Gassmann et al., 2012). In addition, fields in the valley bottoms are drained by a secondary  
81 network of smaller and usually shorter field drains that are either connected to the primary drainage network or directly  
82 connected to the stream (Schuetz et al., 2016). A 20,000 m<sup>3</sup> detention basin was built at the outlet of the Loechernbach to  
83 prevent flooding of the downstream village. Inside the detention basin, a 258 m<sup>2</sup> vegetated surface flow constructed wetland  
84 and a 105 m<sup>2</sup> retention pond (maximum depth 1.5 m) are connected in series parallel to the course of the Loechernbach stream.  
85 A small dam diverts all flow through the vegetated treatment systems during base flow conditions, but allows water to bybass  
86 the VTS during large discharge events. The wetland is in operation since 2010 and its succession was studied by Schuetz et al.  
87 (2012). The pond was added to the system in January 2016. The entire detention basin is sealed by an impermeable clay layer  
88 that prevents leakage to groundwater. Water residence times range from less than one hour during flood events up to several  
89 days during extreme low flow conditions.

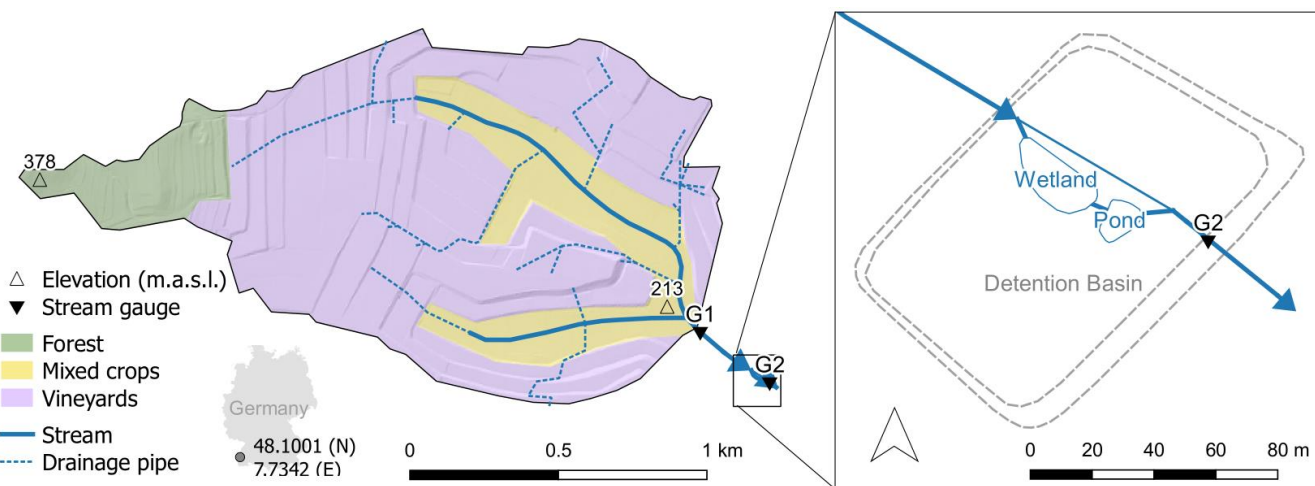


**Figure 1: Loechernbach catchment and vegetated treatment system (VTS) consisting of a vegetated stream reach, a constructed wetland and a retention pond inside a flood detention basin. Shading is based on a digital terrain model with a resolution of 1 m<sup>2</sup>. Location of drainage pipes is according to Gassmann et al. (2012).**

## 2.2 Target compounds

In this study, we focused on 6 target compounds including the fungicides boscalid and penconazole, the herbicides metazachlor and flufenacet, and the TPs metazachlor sulfonic acid (met-ESA) and metazachlor oxalic acid (met-OA). Selected physicochemical properties of the target compounds are listed in Table 1. According to the Pesticide Properties Data Base (Lewis et al., 2016) the contaminants can be classified as low (boscalid) to moderately soluble in water, very mobile (TPs) to slightly mobile (fungicides). The target fungicides are considered moderately fast degradable in the water phase and persistent in soils, while the target herbicides are considered stable in the water phase and non-persistent in soils. TPs of metazachlor are considerably more persistent in soil than their PC. The fungicides are considered stable with respect to hydrolysis but degradable via photolysis, while the herbicides are stable regarding both.

**Table 1: Physicochemical properties of the target compounds according to the Pesticide Properties Data Base (Lewis et al., 2016) including chemical formula, water solubility, organic carbon sorption coefficient (K<sub>OC</sub>) as well as half lives in water (T<sub>50</sub> water) and soil (T<sub>50</sub> soil).**

	<i>Fungicides</i>		<i>Herbicides</i>		<i>TPs</i>	
	Boscalid	Penconazole	Metazachlor	Flufenacet	met-ESA	met-OA
<b>Chemical formula</b>	C <sub>18</sub> H <sub>12</sub> Cl <sub>2</sub> N <sub>2</sub> O	C <sub>13</sub> H <sub>15</sub> Cl <sub>2</sub> N <sub>3</sub>	C <sub>14</sub> H <sub>16</sub> ClN <sub>3</sub> O	C <sub>14</sub> H <sub>13</sub> F <sub>4</sub> N <sub>3</sub> O <sub>2</sub> S	C <sub>14</sub> H <sub>17</sub> N <sub>3</sub> SO <sub>4</sub>	C <sub>14</sub> H <sub>15</sub> N <sub>3</sub> O <sub>3</sub>
<b>Molecular mass (g mol<sup>-1</sup>)</b>	343.2	284.2	277.8	363.3	323.4	273.3
<b>Solubility (mg l<sup>-1</sup>)</b>	4.6	73.0	450.0	51.0	-	-
<b>K<sub>OC</sub> (ml g<sup>-1</sup>)</b>	772.0	2205.0	79.6	273.3	5.0	24.6
<b>T<sub>50</sub> Photolysis (d)</b>	30.0	4.0	stable	stable	-	-
<b>T<sub>50</sub> Hydrolysis (d)</b>	stable	stable	stable	stable	-	-

<b>T<sub>50</sub> Water (d)</b>	5.0	2.0	216.0	54.0	-	-
<b>T<sub>50</sub> Soil (d)</b>	246.0	117.0	10.8	19.7	123.3	90.0

107

### 108 **2.3 Discharge measurement and sampling procedure**

109 Stream flow was measured every minute between April 2016 and September 2017 at two gauges about 200 m upstream of the  
110 treatment system (G1) and at its outlet (G2). Water levels at G1 were recorded inside a 1.37 m standard H-flume (Bos, 1989)  
111 by means of a pressure transducer (Decagon CTD-10) and related to discharge using a standard rating curve. At G2 water  
112 levels were measured in a rectangular cross-section 2 meters ahead of the detention basin outlet by a radar gauge (Vegapuls 61).  
113 The corresponding rating curve for G2 accounted for complete submergence of the control gate valve (Peter, 2005). Pesticide  
114 monitoring at G1 and G2 consisted of 5 manual sample collections during stationary flow conditions and 10 automated event  
115 samplings during discharge events. Event sampling was triggered when a water level increase of more than 3 cm/h was  
116 registered at G1. An automatic sampler (ISCO 3700) started to fill pairs of 900 ml glass bottles at 0, 0.5, 1, 2, 6, and 12 hours  
117 after activation. A second automatic sampler (ISCO 3700) was launched at G2 following the same sampling scheme but with  
118 a time lag of one hour to account for transit between G1 and G2. All samples were recovered from the study site within 24 h  
119 after sampling and cooled until analysis. Sampling was complete except for one case. Due to accident we lost the first sample  
120 of event 9 (2017/10/08 03:30). As concentrations in the first samples were usually very low (Figure 3) and not considered to  
121 markedly influence mass calculation, we assumed that all contaminants in this sample had zero concentration and left this  
122 event in our data set.

### 123 **2.4 Analytical methods**

124 The following analytical methods were used for determining pesticide levels in the water samples. Analytical standards of  
125 boscalid (99.9%), penconazole (99.1%), metazachlor (99.6%), and flufenacet (99.5%) and the internal standards Diuron-D6  
126 (99 %) and Terbutryn-D5 (98.5 %) already dissolved in acetonitrile (100 µg mL<sup>-1</sup>) were purchased from Sigma-Aldrich  
127 Chemie GmbH (Steinheim, Germany). Met-ESA (95 %) and met-OA (98.8 %) were received from Neochema (Bodenheim,  
128 Germany). Acetonitrile (LC-MS grade; VWR International GmbH, Darmstadt, Germany) was used as organic mobile phase  
129 in chromatography and for the preparation of stock solutions. Aqueous mobile phase was prepared with ultrapure water  
130 (Membra Pure, Germany; Q1:16.6 mΩ and Q2: 18.2 mΩ).  
131 Preparation of environmental samples (approx. 1 liter) was done by filtering with a folded filter (type 113 P Cellulose ø 240  
132 mm). Supernatant was spiked with the internal standard Diuron-D6 (10 µl of 10 mg L<sup>-1</sup>). Extraction procedure was a solid  
133 phase extraction (SPE). Cartridges (CHROMABOND® HR-X 6 mL/200 mg) were conditioned with 10 mL methanol and  
134 washed with 10 mL pure water. 90 µL of the extract were spiked with 10 µl of Terbutryn-D5 as an internal standard. Each  
135 sample was a double determination. Measurements of environmental samples were conducted with a Triple Quadrupole  
136 (Agilent Technologies, 1200 Infinity LC-System and 6430 Triple Quad, Waldbronn, Germany). Mobile phases were 0.01%

formic acid (A) and acetonitrile (B) with a flow of 0.4 mL min<sup>-1</sup>. Gradient was as follows: 0-1 min (10% B), 1-11 min (10-50% B), 11-18 min (50-85% B), 18-21 min (85-90% B), 21-24 min (90% B), 24-26 min (90-10% B) and 26-30 (10% B). A NUCLEODUR® RP-C18 (125/2; 100-3 µm C18 ec) column (Macherey Nagel, Düren, Germany) was used as stationary phase with a set oven temperature of T = 30°C. Calibration curve were prepared in pure water. The linearity was evaluated by preparing three curves with ten calibration points in the range 1 - 500 µg/L. The standard curves were then extracted according to the protocol and analyzed using LC-MS/MS. The calculated linear regression values (R<sup>2</sup>) were very good with R<sup>2</sup>-values > 0.999. The linearity between peak area and concentration of substances were obtained in a range of 0 - 5 µg L<sup>-1</sup>. Hence limits of detection (LOD) and quantitation (LOQ) were calculated with DINTEST (2003) according to DIN 32645 considering an enrichment factor of 5000. LOD and LOQ amounted to 0.4 and 1.3 ng L<sup>-1</sup> (boscalid), 0.3 and 0.9 ng L<sup>-1</sup> (penconazole), 0.3 and 1.2 ng L<sup>-1</sup> (metazachlor), 0.4 and 1.3 ng L<sup>-1</sup> (flufenacet) as well as 0.6 and 2.2 ng L<sup>-1</sup> (met-ESA) and 0.5 and 1.6 ng L<sup>-1</sup> (met-OA) considering an enrichment factor of 5000. A detailed analysis of measurement precision can be found in the supplementary material (Text S1).

## 2.5 Data analysis and calculations

2.5.1 Identification of patterns in input concentration  
Identification of patterns in input chemographs was done by k-medoids cluster analysis - a variation of the commonly applied k-means algorithm. Both approaches partition the elements of a dataset into a predefined number k of clusters by attributing the elements to the cluster with the nearest cluster center. Optimal clustering is achieved by iteratively updating cluster centers and minimizing distance between data points and cluster centers. K-medoids differs from k-means as it uses existing points (medoids) as cluster centers instead of means and is considered more robust against extreme values and outliers (Han et al., 2012). A total of 58 concentration sequences was included in the analysis, consisting of 10 sequences per target compound, except for flufenacet which did not exceed LOQ in two events. Prior to cluster analysis, data was normalized by the maximum of each chemograph to promote that clustering represented shape, rather than differences in absolute concentration. The analysis was done using the software R (R Core Team, 2019) (version 3.6.1) using the ‘pam’ (partitioning around medoids) function from the ‘cluster’-package (version 2.1.0) (Maechler et al., 2019). We tested clustering for k ranging between 2 and 10, the final number was determined by both visual inspection of the clusters and assessment of explanatory benefit per additional cluster (elbow method). As a result we found that k=4 resulted in the best partition.

## 2.5.2 Contaminant mitigation

Contaminant retention was assessed in terms of both peak-concentration reduction rate (R<sub>C</sub>) and mass removal rate (R<sub>M</sub>). R<sub>C</sub> was calculated in accordance with other studies (Eq. 2), e.g. Elsaesser et al. (2011), Stehle et al. (2011) and Passeport et al. (2013):

$$R_C = \frac{C_{in,max} - C_{out,max}}{C_{in,max}} \cdot 100 \% , \quad (1)$$

167 where  $C_{in,max}$  and  $C_{out,max}$  are peak concentrations registered at the inlet and outlet sampling points, respectively.  $R_M$  was  
 168 calculated analogously from the input ( $M_{in}$ ) and output contaminant mass ( $M_{out}$ ):

$$R_M = \frac{M_{in} - M_{out}}{M_{in}} \cdot 100 \% , \quad (2)$$

169 Contaminant masses were calculated from discharge at G1 and G2 and linearly interpolated contaminant concentrations. As  
 170 water level data from G2 showed evidence for inaccuracy during low flows as result of the rectangular shape of the measuring  
 171 cross-section at G2, we did not assess mass removal during stationary flow conditions. As we did not sample the wetland  
 172 sediments or plants, the mass removal rate calculated following the above procedure describes the relative difference of  
 173 dissolved contaminant mass entering and leaving the wetland within the duration of the sampling procedure. It is therefore not  
 174 independent of the wetland's water balance:

$$W_B = \frac{Q_{in,mean} - Q_{out,mean}}{Q_{in,mean}} \cdot 100 \% , \quad (3)$$

175 where  $Q_{in,mean}$  and  $Q_{out,mean}$  are the discharge at G1 and G2, respectively, averaged over the duration of the sampling procedure  
 176 at both gauges.  $W_B$  was positive, if more water entered the wetland than left the wetland during the sampling procedure, and  
 177 negative in the opposite case.

### 178 2.5.3 Dispersion sensitivity of chemographs

179 We defined a dispersion sensitivity index as follows:

$$i_{DS} = \frac{C_{in,max} - C_{in,n}}{C_{in,max}} , \quad (4)$$

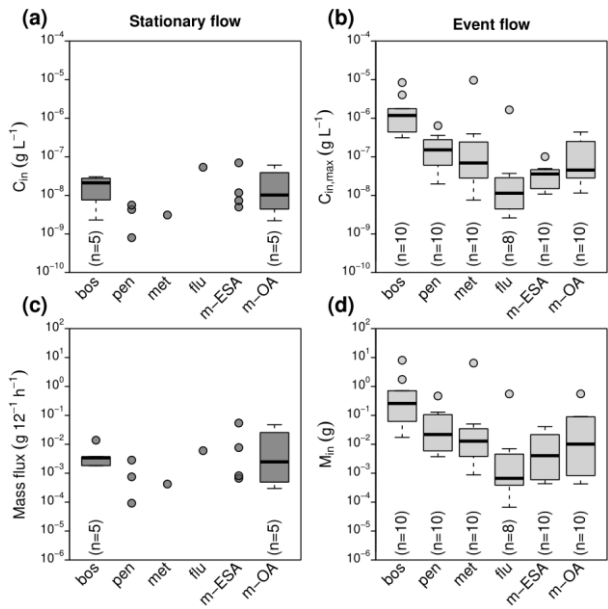
180 where  $C_{in,n}$  is the concentration in the last sample and  $C_{in,max}$  is the peak concentration of a chemograph recorded at the inlet of  
 181 the VTS (G1). In other words,  $i_{DS}$  represents the fraction of the concentration peak that can potentially be flattened by  
 182 dispersion.

## 183 3 Results

### 184 3.1 Contaminant mobilization

185 Contaminant concentrations in stream water (G1) differed clearly depending on the flow conditions (Figure 2). During  
 186 stationary flow, concentrations of boscalid and the TPs of metazachlor ranged in the order of tens of nanograms, while  
 187 penconazole, metazachlor and flufenacet only occasionally exceeded the LQ. During discharge events in contrast, peak  
 188 concentrations varied from a few nanograms (flufenacet) to several milligrams per liter (boscalid) spanning a range of 6 orders  
 189 of magnitude. Concentration increase during events compared to stationary flow was different among the compounds. Median  
 190 concentration of boscalid increased by a factor of 48, while concentrations of met-ESA and met-OA only increased by a factor  
 191 of 3 and 5, respectively. Similar patterns were found for contaminant mass. Contaminant mass mobilized in the catchment  
 192 during discharge events ranged from several hundreds of micrograms (flufenacet) to several hundreds of milligrams (boscalid)

193 and even several grams in exceptional cases (boscalid, metazachlor). Based on compound medians, about 76 times more  
194 boscalid but only about 4 times more met-OA were transported during discharge events than during an equally long period  
195 under stationary flow conditions.

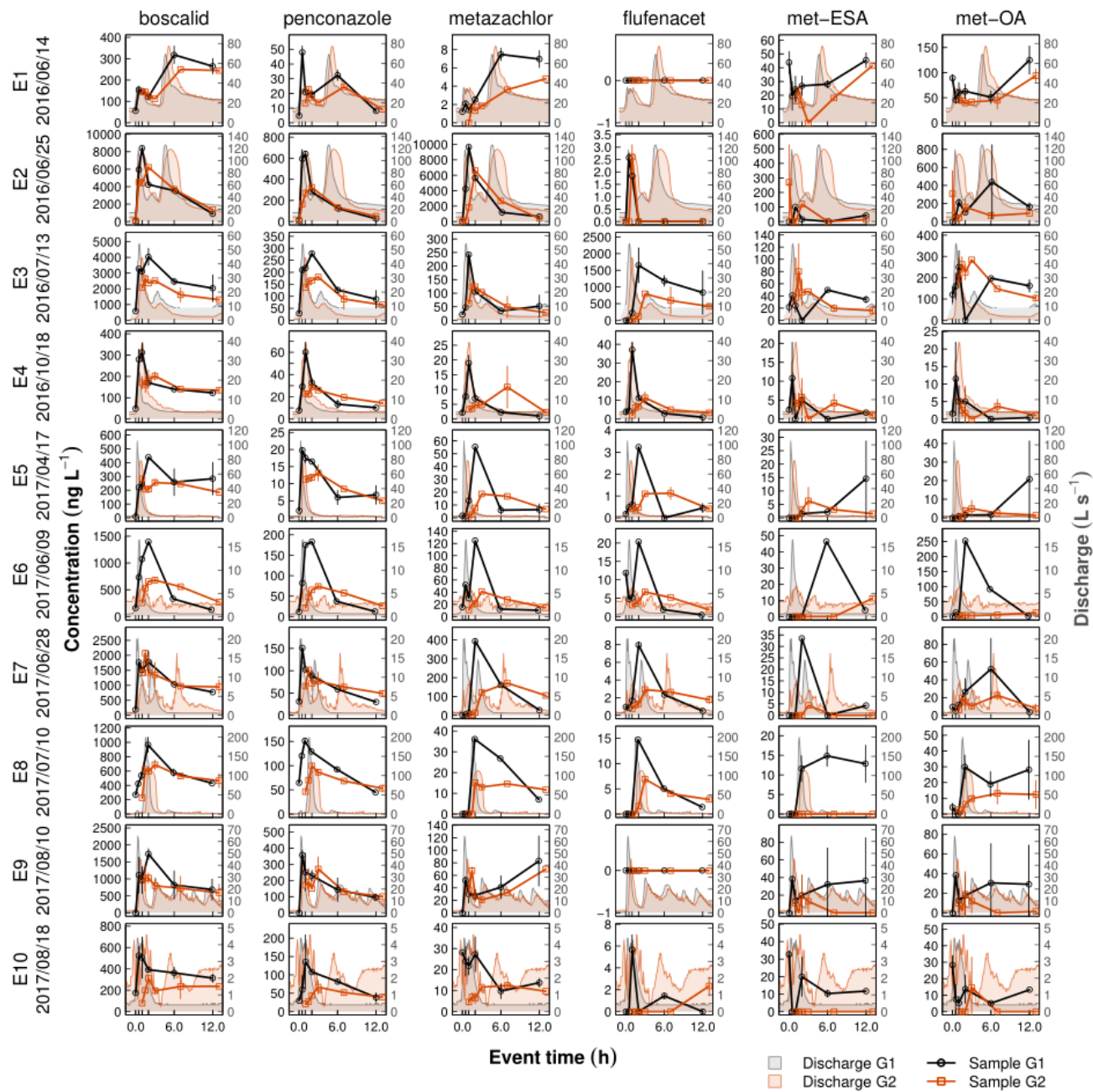


196  
197 **Figure 2: Peak concentrations at G1 during stationary flow (a) and flow events (b) as well as contaminant mass flux during stationary**  
198 **flow (c) and transported mass per event (d). Boxplots indicate median and interquartile range (IQR). Whiskers indicate extreme**  
199 **points within 1.5 times the IQR from the boxes, circles indicate points outside this range.**

200 The 10 events were characterized by different discharge magnitudes and dynamics (Figure 3). Mean discharge during the  
201 events ranged between 0.7 (E10) and 32.0 L s<sup>-1</sup> (E2) with respective peak values between 4.4 (E10) and 199.7 L s<sup>-1</sup> (E2). The  
202 recorded event hydrographs included events with one single discharge peak (E4, E5, E6, E10), with one major peak followed  
203 by one or more secondary peaks (E2, E3, E7, E9), and events in which a major peak followed an earlier smaller peak (E1, E8).  
204 In most cases discharge had recessed to pre-event levels by the end of the 12-hour sampling procedure, only E1 and E2 showed  
205 ongoing flow recession. In many cases, concentrations in the final event samples were still elevated compared to pre-event



206 conditions. However, due to flow recession, mass flux was usually very low by the time the last sample was collected  
207 (Figure S1).



208  
209 **Figure 3: Contaminant concentration at the inlet gauge G1 and the outlet gauge G2 of the 6 target compounds during 10 discharge**  
210 **events. Data points represent means of duplicate samples and standard deviation (error bars).**

### 212 3.2 Patterns in chemographs

213 Cluster A (Figure 4) was characterized by absence of a clear peak during the first two hours of sampling but elevated  
214 concentrations during later times, resulting in low  $i_{DS}$ . Cluster B showed a quick response, i.e. concentrations increased sharply  
215 within the first 30 minutes. Concentrations were the highest of all clusters and still elevated in the last sample compared to  
216 pre-event levels. Cluster C was characterized by a clear peak within the first two hours and a low tailing and was the cluster  
217 with highest median  $i_{DS}$ . Cluster D showed the most inconsistent pattern and maximum concentrations appeared later compared  
218 to clusters B and C. A relatively clear pattern was evident in the attribution of compounds to the clusters. Chemographs of the  
219 fungicides boscalid and penconazole were mainly assigned to cluster B, while the herbicides and the TPs were assigned to the  
220 remaining three clusters. Cluster A was composed of herbicide and TP chemographs, particularly from events with multiple  
221 discharge peaks. Cluster D represented chemographs of herbicides and TPs mainly during the events E5 to E8 which were all  
222 characterized by sharp discharge peaks during periods of generally low flow (Figure 3). Almost all chemographs of the events  
223 E2 and E4 were attributed to cluster C.

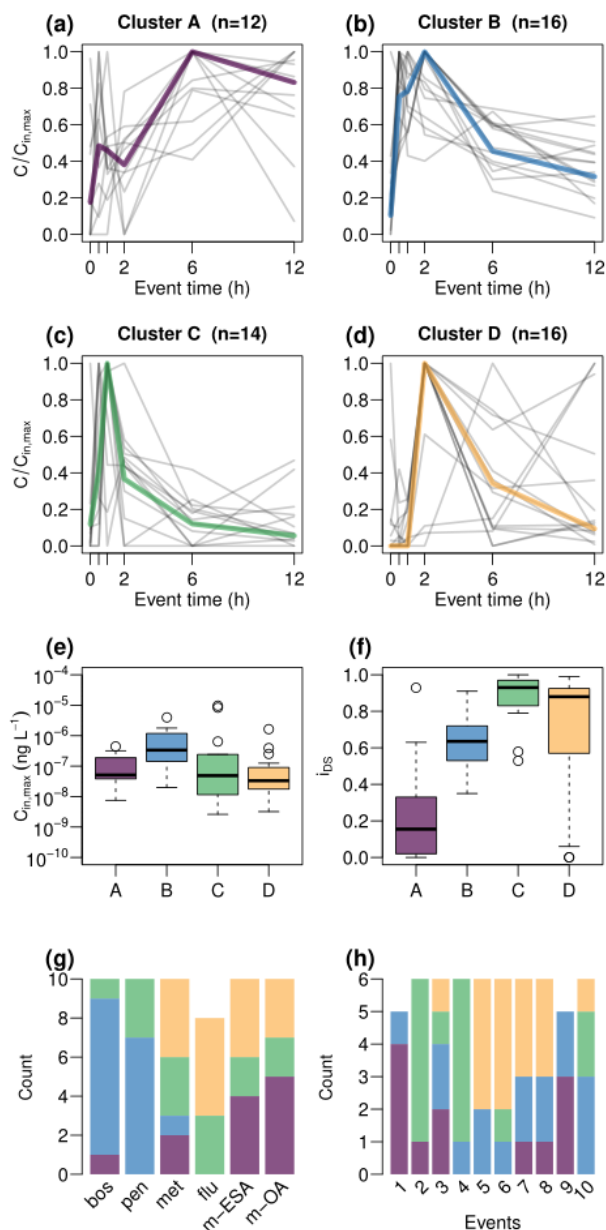


**Figure 4: Clustered event chemographs as well as maximum input concentration, dispersion sensitivity index, and attribution of compounds and events to the different clusters**

### 3.3 Contaminant mitigation in the wetland

Contaminants were mitigated in the wetland in terms of both  $R_C$  (Eq.1) and  $R_M$  (Eq.2).  $R_C$  (Figure 5a) was close to zero for boscalid and poorly constrained for the remaining compounds during stationary conditions, partly due to insufficient number of detections. During discharge events, in contrast, peak concentrations of all compounds were clearly reduced. While  $R_C$  was narrowly constrained for the fungicides and herbicides, TPs exhibited higher variability. Mean  $R_C$  and corresponding standard

232 deviations were  $29.8 \pm 18.4$  % (boscalid),  $42.1 \pm 11.5$  % (penconazole),  $47.9 \pm 16.4$  % (metazachlor),  $53.8 \pm 22.6$  %  
 233 (flufenacet),  $29.5 \pm 84.7$  % (met-ESA), and  $47.9 \pm 29.5$  % (met-OA), respectively.  $R_C$  was clearly different among chemograph  
 234 clusters with lowest values in cluster A and highest values in cluster D (Figure 5b). Moreover,  $R_C$  was higher for the lower  
 235 half of peak concentrations than for the upper half (Figure 5c) and systematically increased with dispersion sensitivity (Figure  
 236 5d).  $R_C$  was also related to discharge conditions. Highest  $R_C$  values were reached, when mean discharge was low (Figure 5e)  
 237 but the ratio of maximum to mean discharge was elevated (Figure 5f), i.e. in events characterized by low pre-event discharge  
 238 and sharp discharge peaks (in particular events attributed to cluster D in Figure 4). Although there was evidence for major  
 239 water surpluses and deficits in the event water balance between G1 and G2, particularly in events with low discharge such as  
 240 events E6 and E10, an imbalanced water balance had only minor effects on  $R_C$  (Figure 5g). We did not find clear relationships  
 241 between  $R_C$  and compound properties such as  $K_{fOC}$ , water solubility or soil half-live (Figure 5h-j).  
 242 Relative mass removal during discharge events (Figure 6a) resulted in smaller rates and higher variability compared to  $R_C$ .  
 243 Mean  $R_M$  and corresponding standard deviations were  $7.7 \pm 29.6$  % (boscalid),  $17.3 \pm 26.0$  % (penconazole),  $18.1 \pm 27.8$  %  
 244 (metazachlor),  $27.0 \pm 28.1$  % (flufenacet),  $35.2 \pm 68.4$  % (met-ESA), and  $44.0 \pm 28.7$  % (met-OA). These values show that  
 245 mass removal was limited for most compounds. Although the general pattern in  $R_M$  for the different compounds was similar  
 246 to  $R_C$ , behavior of  $R_M$  among the chemograph clusters was different. While  $R_C$  increased from cluster A to cluster B and C,  
 247  $R_M$  decreased (Figure 6b). Cluster D exhibited high values of both  $R_C$  and  $R_M$ . No clear response was found to different levels  
 248 of input mass (Figure 6c), however, median  $R_M$  was lowest when peaks in chemographs were sharpest (Figure 6d). This means  
 249 the relationship of  $R_M$  to increasing sharpness of chemograph peaks was inverted compared to  $R_C$ .  $R_M$  was not obviously  
 250 related to discharge dynamics, neither to mean discharge (Figure 6e), nor to the ratio of maximum to mean discharge (Figure  
 251 6f). Disregarding events with very low discharge (events E6 and E10), it seemed possible that much of  $R_M$  was the result of  
 252 water imbalances during the events (Figure 6g). However,  $R_M$  of most chemographs plotted above the 1:1 line of  $R_M$  and  
 253 relative water balance, indicating that  $R_M$  was higher than water imbalance would explain.  $R_M$  showed a tendency to decrease  
 254 with increasing  $K_{fOC}$  (Figure 6h), but no clear pattern was found for solubility (Figure 6i) and soil half-live (Figure 6j).

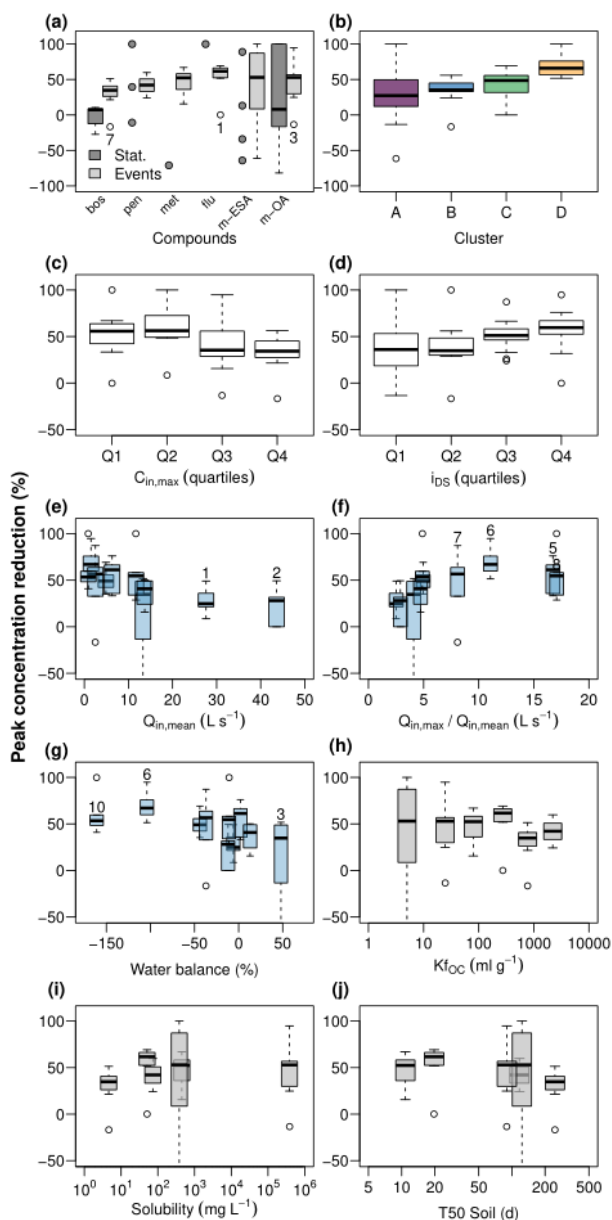


**Figure 5** Contaminant peak concentration reduction in the wetland (a) during stationary and event flow conditions and its relationship to chemograph properties, discharge conditions, and physiochemical properties of the target compounds. Chemograph properties include clustering (b), peak concentrations (c), and ratio of concentrations during the peak and in the tailing (d). Discharge conditions include mean discharge at G1 (e), ratio of maximum to mean discharge at G1 (f), and water balance between G1 and G2 (g). Event numbers are shown for selected events. Compound properties include organic carbon sorption coefficient (h), solubility in water (i) and soil half-live (j).

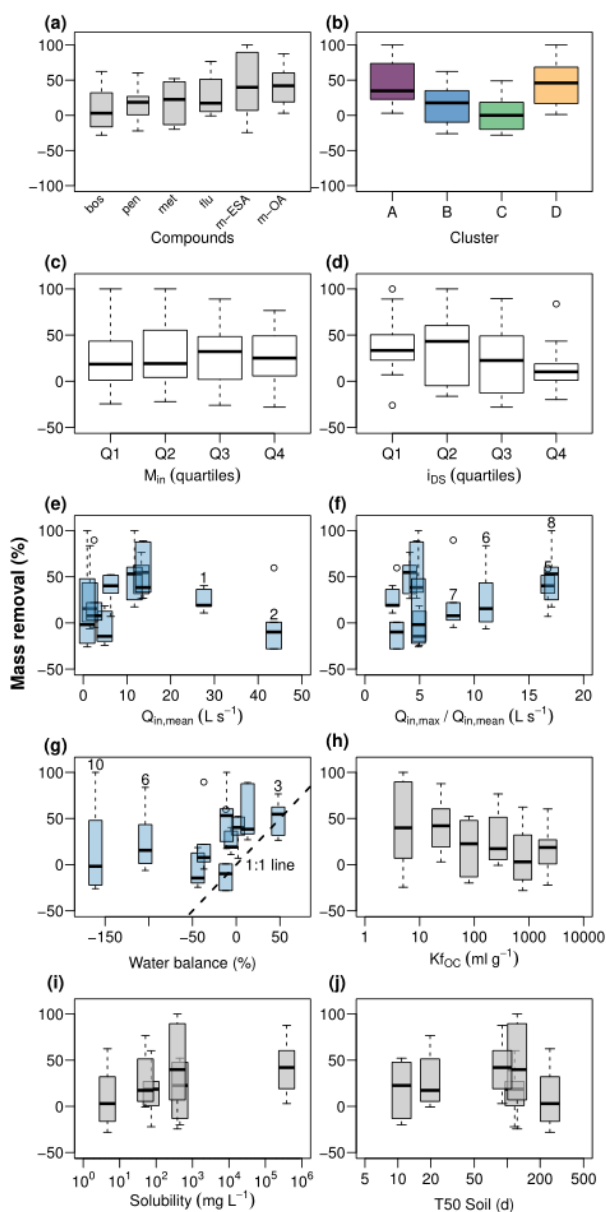


**Figure 6: Contaminant mass removal in the wetland (a) during event flow conditions and its relationship to chemograph properties, discharge conditions, and physiochemical properties of the target compounds. Chemograph properties include clustering (b), peak concentrations (c), and ratio of concentrations during the peak and in the tailing (d). Discharge conditions include mean discharge at G1 (e), ratio of maximum to mean discharge at G1 (f), and water balance between G1 and G2 (g). Event numbers are shown for selected events. Compound properties include organic carbon sorption coefficient (h), solubility in water (i) and soil half-live (j).**

## 268 4 Discussion

### 269 4.1 Monitoring setup and associated uncertainties

270 Regarding chemographs and calculation of  $R_C$ , uncertainties arose from timing and frequency of sampling and analytical error,  
271 and additionally from discharge measurement when calculating masses and  $R_M$ . Analytical methods used in this study usually  
272 produced very consistent results so that variability in concentrations of parent compounds in duplicate samples was low  
273 ( $sd < 10\%$ ). However, in individual samples collected at G1 analytical variability was elevated for met-ESA and met-OA  
274 (Figure 3), reducing confidence in concentrations and the derived measures  $R_C$  and  $R_M$  of TPs in the affected chemographs  
275 (E2, E5, E7, E8, E9). Uncertainty related to timing and frequency of sampling can hardly be quantified but certainly depends  
276 on how well the sampling intervals captured variability in concentrations during flood events and how well the time lag  
277 between upstream and downstream sampling matched the residence time of solutes in the wetland. Lefrancq et al. (2017)  
278 assessed the effect of sampling frequency in pesticide monitoring data collected during runoff from a single vineyard and  
279 found that acute toxicity of pesticide flushes was underestimated up to 4-times when calculated from event means and up to  
280 30-times when calculated from random samples. Although these data were collected on the plot scale and we assume that  
281 variability in our catchment is lower due to longer flow paths and mixing processes on the catchment scale, uncertainty of the  
282 chemographs in our study could have been reduced by increasing sampling frequency. Regarding the timing of upstream and  
283 downstream sampling, there is evidence that water residence time in the wetland was in fact shorter than one hour. The  
284 observation that for quickly responding compounds, such as boscalid, concentration in the first sample at G2 was often elevated  
285 compared to the first sample at G1 indicates that the contaminant flush had already reached G2 when sampling started. This  
286 did not influence determination of  $C_{out,max}$  and  $R_C$  in the outlet of the wetland, as concentrations were still rising from the first  
287 to the second sample (Figure 3). However, effects on  $M_{out}$  were higher, since a relevant fraction of contaminant mass leaving  
288 the wetland was not registered and thereby caused overestimation of  $R_M$  (Figure S1). Another source of uncertainty exclusively  
289 affecting contaminant mass and not concentrations was the use of different gauging systems at G1 and G2. Different shapes  
290 of the measurement cross-section (triangular at G1 and rectangular at G2) caused G2 to be less precise and water imbalances  
291 on the event scale, particularly when flow was low. Summarizing the setup constraints above, we have high confidence that  
292 the experimental setup produced realistic chemograph shapes and captured peak concentration reasonably well, but are less  
293 confident regarding contaminant loads.

### 294 4.2 Mobilization of contaminants and formation of distinct chemographs

295 Peak concentrations of mobilized contaminant flushes were different depending on the compound. This may be due to the  
296 application of different amounts and due to temporal patterns of application. The fact that maximum concentrations of  
297 metazachlor and flufenacet in specific events exceeded concentrations during most other events by a factor of more than 100,  
298 suggested application of these compounds shortly before the onset of runoff. Despite highly variable application patterns, our  
299 cluster analysis resulted in four groups with similar chemograph shape. Many factors have been shown in literature to influence  
300 the mobilization of pesticides in catchments, including catchment properties, event properties and physiochemical compound

properties. As catchment properties we here consider factors associated with runoff generation such as catchment geometry, terrain slopes, and in particular the delineation of areas where different compounds were applied. The interplay of these factors defines hydrological activity and connectivity (i.e. by shortcuts like roads and drainage pipes) of critical source areas for different compounds (Doppler et al., 2012; Gomides Freitas et al., 2008). Event properties include intensity and dynamics of rainfall (Imfeld et al., 2020) and subsequent runoff (Doppler et al., 2014). Relevant physiochemical compound properties are e.g. mobility and degradability (Gassmann et al., 2015).

These properties are reflected to varying degrees in the results of the cluster analysis. Cluster A was characterized by a quick response and a concentration plateau towards the end of sampling and was mainly composed of TPs. The fact that concentration maxima in cluster A were delayed compared to fungicides (cluster B), although their parent compounds were applied closer to the stream in the flat valley bottoms, suggests that they were transported with a slower flow components. Due to flatter terrain, surface runoff played a less important role and the main transport pathway was subsurface flow. Where fields were undrained, however, transit time of water from the infiltration point to the stream would likely exceed the temporal scale of event sampling. Most of the water reaching the stream from the fields in the valley during discharge events would therefore be pre-event water, enriched in TPs formed in the soil, corresponding to the formation site of TPs of the chloracetamide herbicides to which metazachlor belongs (Mersie et al., 2004). Seepage of pre-event TP-rich water thus explains the immediate response of chemographs in cluster A. The quick response was often followed by a local concentration minimum between samples 2 and 5, i.e. between 30 min and 6 h after sampling was initialized. Coincidence of this minimum with concentration peaks of fungicides might suggest dilution of TP concentration by mixing with event water carrying high loads of fungicides but less TPs of metazachlor.

Cluster B represented differences between fungicides and the remaining compounds. Considering land use distribution in the studied catchment, it is unclear whether this partition reflects different compound properties or catchment properties or both. The fact that concentration in cluster B quickly increased with discharge (within 30 minutes) is in line with fast transport from the vineyard terraces to the stream via roads and drainage pipes as described by Gassmann et al. (2012) for suspended solids in the studied catchment. Along such preferential pathways, compound properties, such as sorption affinity, may be less important (Gomides Freitas et al., 2008) compared to e.g. percolation through the soil with intense contact to sorption sites in the soil matrix. Moreover, fungicides are applied by sprayers into the foliage and can drift to e.g. paved surfaces from which they can be quickly mobilized by subsequent rainfall (Lefrancq et al., 2013). We therefore hypothesize that cluster B was mainly produced by surface flushing and fast transport pathways of fungicides. This explained the quick rise and subsequent decline in concentrations (concurrent with plateaus produced by slower flow components in cluster A).

Cluster C was composed of chemographs of all compounds but mainly from events E2 and E4 indicating event dependence. Two aspects were found to support this idea. First, there was a secondary discharge peak in event 2 that did not contribute much in terms of contaminant concentration but rather caused dilution and produced particularly flat chemograph tails. Second, peaks of herbicides and TPs were less delayed compared to fungicides. This may be the result of recent herbicide application and active surface runoff in the flat valleys. Timing of pesticide application was identified as the main export driver of currently



used pesticides by Imfeld et al. (2020) who performed a cluster analysis on rainfall data from a headwater vineyard catchment. Based on the magnitude of discharge and amount of mobilized contaminants (concentration of metazachlor  $\approx 10 \mu\text{g L}^{-1}$ ), both explanations seem plausible in event E2. Event E4, however, did not show particularly high herbicide concentration nor a secondary discharge peak. Although it is obvious that chemograph shapes in cluster C differed from the other clusters, unfortunately, the responsible factors remain unclear.

Cluster D included chemographs of both herbicides and TPs and presented a clear peak that was often defined by a single sample 2 h after the beginning of the event. In contrast to cluster A, cluster D was characterized by a single sharp discharge peak (except in event E7 where a second peak occurred shortly after the first) and mainly included chemographs during periods of low flow. Our interpretation is that cluster D represented flow events in which no dilution of herbicide and TP fluxes by fungicide fluxes or secondary discharge peaks occurred. Low pre-event discharge in cluster D compared to cluster A may indicate low water levels which may have caused a slower response as no enriched pre-event water was released from the soils in the valleys.

The unclear interpretation of cluster C suggest that we missed important factors for the formation of chemographs. In fact, variables like spatial distribution of rainfall or pesticide application rates and timing (Imfeld et al., 2020) and possibly other factors likely influenced chemograph shapes. Knowing all these variables would not change the results produced by the clustering algorithm but rather increase our ability to interpret them. Nevertheless, the cluster analysis helped to explore how the catchment and processes therein influenced concentration signals of mobilized contaminants. Particularly, the analysis helped to understand under what conditions and for which pollutant sharp-peaked chemographs, associated with high acute toxicity, can be expected. We therefore see a high potential of this type of analysis for the identification of influential factors for contaminant mobilization in other catchments, although these factors may not be universal but catchment-dependent.

### **4.3 Mitigation efficiency and chemograph shape**

#### **4.3.1 Peak concentration reduction**

We hypothesized that peak concentration reduction in the VTS will be highest for chemographs with the sharpest peaks, i.e. for the chemographs that were most sensitive to dispersion. And indeed we found a systematic relationship between  $R_C$  and both  $i_{DS}$  and chemograph clusters. Although the relationship of clusters and  $R_C$  largely reflected the relationship between  $R_C$  and  $i_{DS}$ , it is surprising that  $R_C$  was clearly highest in cluster D and not in cluster C which presented better defined peaks and slightly higher  $i_{DS}$  per cluster (Figure 4f). Critical inspection of input chemographs shows that in several chemographs of TPs (met-ESA and met-OA in event E4 and met-OA in event E8) elevated concentrations in the last samples exhibited high analytical errors and did not appear in the outlet chemograph. These dubious samples caused low  $i_{DS}$  but substantial  $R_C$  and thus contributed to variability in  $i_{DS}$  despite high values of  $R_C$  in cluster D. We therefore do not consider the deviation from the expected cluster ordering contradictory but to result from increased uncertainty in cluster D as mentioned earlier. In contrast, the hypothesized relationship between  $R_C$  and chemograph shape was demonstrated for both  $i_{DS}$  and chemograph

clusters, the latter of which also integrates shape aspects that go beyond  $i_{DS}$ , e.g. timing of peaks. Overall, the values of  $R_C$  found in our study compare with field data from vegetated buffers (Bundschuh et al., 2016; Stehle et al., 2011) and are in the range of those found in vegetated stream mesocosms by Elsaesser et al. (2011) and Stang et al. (2014) who both attributed most of the observed peak reduction to dispersion.

In addition, we found relationships between  $R_C$  and discharge dynamics, i.e.  $Q_{mea}$  and ratio of  $Q_{max}$  to  $Q_{mean}$ . The influence of discharge on  $R_C$  may be two-fold. First, increasing flow reduced residence time and hydraulic efficiency, i.e. short circuiting reduced the potential for dispersion and interaction with wetland sediments or plants. Second, the fact that chemographs of events with high  $Q_{max}$  to  $Q_{mean}$  ratios were attributed to cluster D suggests that discharge dynamics influenced the shape of the chemograph at the wetland inlet. This means, the influence of discharge may also be indirect by promoting the formation of sharp-peaked chemographs with high potential for peak reduction.

In contrast to other studies, we did not find clear relationships of  $R_C$  to and physiochemical properties of compounds such as sorption affinity (Stehle et al., 2011; Vymazal and Březinová, 2015) or solubility (Bundschuh et al., 2016). The absence of such relationships may partially be due to the low number of different target compounds in our study ( $n=6$ ). However, given the short time lag between sampling at the inlet and outlet of the wetland ( $\Delta t = 1h$ ), it seems logical that no relevant sorption or degradation occurred within this period. For comparison, in batch experiments by Gaullier et al. (2018) adsorption equilibrium for boscalid (compound with second highest  $K_{fOC}$  in our study) was only reached after 24 h. Despite the relatively narrowly confined  $R_C$  values of the parent compounds, we do not consider physiochemical compound properties as major drivers of  $R_C$  in our VTS.

#### 4.3.2 Contaminant mass removal

For  $R_M$  we found a different pattern among the chemograph clusters than for  $R_C$ .  $R_M$  was apparently higher in clusters A and D than in clusters B and C. However, the clusters indicating substantial mass removal were those with increased uncertainty regarding compound mass. Cluster A often showed relevant mass flux at the end of sampling (and presumably beyond) which we did not account for. Cluster D contained dubious data points of TPs and poorly defined peaks outside the periods of high sampling frequency. In addition, due to overestimation of solute travel time in the wetland in the monitoring setup, the rising limb of the mass flux signal at G2 was often not adequately captured by the sampling scheme, causing underestimation of downstream event mass and overestimation of mass loss. In absence of any clear relationship with compound properties, discharge dynamics or chemograph shape, this suggests that the assessment of contaminant masses was subject to systematical errors and that the apparent mass loss found in our study should therefore not be over-interpreted.

In earlier studies, Lange et al. (2011) and Schuetz et al. (2012) observed a 15-30 % mass loss of the fluorescent tracer sulforhodamine-B in the wetland subsection of the current VTS. These results indicate a general potential for sorption of organic compounds in this system, but represent an earlier succession state of the wetland and stationary flow conditions with much longer residence times. Also in the current VTS kinetic sorption of contaminants may have occurred but sorption equilibrium was certainly not reached (Gaullier et al., 2018). Thus the effect of sorption did not reach its full potential. In fact,

other studies reported limited mass removal in wetlands with comparable residence times. Ramos et al. (2019) did not find relevant  $R_M$  in two surface flow wetlands with residence times between 45 min and 6 h in England. In contrast, Passeport et al. (2013) found  $R_M$  between 45 % and 96 % in a constructed wetland with a residence time of 66.5 h. However, their contaminant mass loss coincided with loss of water (45 %). Mesocosm experiments by Elsaesser et al. (2011) and Stang et al. (2014) showed strong concentration reduction but only very limited and temporary mass removal at residence times of a few hours. In summary, these findings suggest that the potential for mass removal in wetland systems like the one studied here is rather limited. However, wetlands have been shown to reduce contaminant mass, when residence times are sufficiently long (Gregoire et al., 2009) or when operated in batch mode (Tournebize et al., 2017; Moore et al., 2000; Maillard et al., 2016).

#### 4.4 Conclusions

In agreement with other studies this investigation shows that VTSs with short water residence times of up to several hours may cause substantial reduction of peak concentrations of contaminants mobilized during discharge events. This implies an efficient reduction of acute toxicity for receiving aquatic ecosystems. In the present VTS the reduction of concentration peaks was mainly controlled by dispersion and was more pronounced for sharp-peaked than for flat input chemographs. In contrast, contaminant mass loss was rather limited, mainly due to the fact that short residence times did not allow for considerable sorption or transformation. Clustering of chemographs revealed that chemograph shapes were associated with source areas, input pathways and discharge dynamics. This highlighted the role of chemographs as links between processes in catchments and in receiving aquatic systems. The presented cluster analysis helped to understand why and for which pollutant sharp-peaked chemographs could be expected. Such sharp-peaked chemographs produce high acute toxicity in aquatic ecosystems but at the same time can efficiently be mitigated in VTSs. While the factors controlling chemograph shape may be different in different catchments, the effect dispersion exerts on these signals is universal.

#### Data availability

Contaminant data used in this study is available as supplementary material.

#### Author contributions

JL planned the monitoring concept. JG performed the data analysis and prepared most of the manuscript in cooperation with JL. . OO and KK facilitated the sample analysis and OO wrote the section on analytical methodology.

#### Competing interests

The authors declare that they have no conflict of interest.

## 427 Financial support

428 This research has been supported by the Federal Ministry of Education and Research (BMBF) (grantno. 02WRM1366B) and  
429 the Water Network Baden-Württemberg funded by the Ministry of Science, Research and Art of the State of Baden-  
430 Württemberg. The article processing charge was funded by the Baden-Wuerttemberg Ministry of Science, Research and Art  
431 and the University of Freiburg in the funding program Open Access Publishing.

432

## 433 References

- 434 Aubert, A. H. and Breuer, L.: New seasonal shift in in-stream diurnal nitrate cycles identified by mining high-  
435 frequency data, PLoS One, 11, e0153138, doi:10.1371/journal.pone.0153138, 2016.
- 436 Beketov, M. A., Kefford, B. J., Schäfer, R. B., and Liess, M.: Pesticides reduce regional biodiversity of stream  
437 invertebrates, Proc. Natl. Acad. Sci. USA, 110, 11039–11043, doi:10.1073/pnas.1305618110, 2013.
- 438 Bos, M. G. (Ed.): Discharge measurement structures, International Institute for Land Reclamation and  
439 Improvement, Wageningen, The Netherlands, 1989.
- 440 Bundschuh, M., Elsaesser, D., Stang, C., and Schulz, R.: Mitigation of fungicide pollution in detention ponds and  
441 vegetated ditches within a vine-growing area in Germany, Ecol. Eng., 89, 121–130,  
442 doi:10.1016/j.ecoleng.2015.12.015, 2016.
- 443 Doppler, T., Camenzuli, L., Hirzel, G., Krauss, M., Lück, A., and Stamm, C.: Spatial variability of herbicide  
444 mobilisation and transport at catchment scale: insights from a field experiment, Hydrol. Earth Syst. Sci., 16,  
445 1947–1967, doi:10.5194/hess-16-1947-2012, 2012.
- 446 Doppler, T., Lück, A., Camenzuli, L., Krauss, M., and Stamm, C.: Critical source areas for herbicides can change  
447 location depending on rain events, Agr. Ecosyst. Environ., 192, 85–94, doi:10.1016/j.agee.2014.04.003,  
448 2014.
- 449 Elsaesser, D., Blankenberg, A.-G. B., Geist, A., Mæhlum, T., and Schulz, R.: Assessing the influence of  
450 vegetation on reduction of pesticide concentration in experimental surface flow constructed wetlands:  
451 Application of the toxic units approach, Ecol. Eng., 37, 955–962, doi:10.1016/j.ecoleng.2011.02.003, 2011.
- 452 Fenner, K., Canonica, S., Wackett, L. P., and Elsner, M.: Evaluating pesticide degradation in the environment:  
453 Blind spots and emerging opportunities, Science, 341, 752–758, 2013.
- 454 Fernández, D., Voss, K., Bundschuh, M., Zubrod, J. P., and Schäfer, R. B.: Effects of fungicides on decomposer  
455 communities and litter decomposition in vineyard streams, Sci. Total Environ., 533, 40–48,  
456 doi:10.1016/j.scitotenv.2015.06.090, 2015.
- 457 Fischer, H. B., List, J. E., Koh, C. R., Imberger, J., and Brooks, N. H.: Mixing in inland and coastal waters,  
458 Academic Press, San Diego, California, 302 pp., 1979.
- 459 Gassmann, M., Lange, J., and Schuetz, T.: Erosion modelling designed for water quality simulation, Ecohydrol.,  
460 5, 269–278, doi:10.1002/eco.207, 2012.
- 461 Gassmann, M., Olsson, O., Stamm, C., Weiler, M., and Kümmerer, K.: Physico-chemical characteristics affect  
462 the spatial distribution of pesticide and transformation product loss to an agricultural brook, Sci. Total  
463 Environ., 532, 733–743, doi:10.1016/j.scitotenv.2015.06.068, 2015.
- 464 Gassmann, M., Stamm, C., Olsson, O., Lange, J., Kümmerer, K., and Weiler, M.: Model-based estimation of  
465 pesticides and transformation products and their export pathways in a headwater catchment, Hydrol. Earth  
466 Syst. Sci., 17, 5213–5228, doi:10.5194/hess-17-5213-2013, 2013.

467 Gaullier, C., Dousset, S., Billet, D., and Baran, N.: Is pesticide sorption by constructed wetland sediments  
 468 governed by water level and water dynamics?, *Environ. Sci. Pollut. Res. Int.*, 25, 14324–14335,  
 469 doi:10.1007/s11356-017-9123-1, 2018.

470 Gomides Freitas, L., Singre, H., Müller, S. R., Schwarzenbach, R. P., and Stamm, C.: Source area effects on  
 471 herbicide losses to surface waters—A case study in the Swiss Plateau, *Agric. Ecosyst. Environ.*, 128, 177–  
 472 184, doi:10.1016/j.agee.2008.06.014, 2008.

473 Gregoire, C., Elsaesser, D., Huguenot, D., Lange, J., Lebeau, T., Merli, A., Mose, R., Passeport, E., Payraudeau,  
 474 S., Schütz, T., Schulz, R., Tapia-Padilla, G., Tournebize, J., Trevisan, M., and Wanko, A.: Mitigation of  
 475 agricultural nonpoint-source pesticide pollution in artificial wetland ecosystems, *Environ. Chem. Lett.*, 7,  
 476 205–231, doi:10.1007/s10311-008-0167-9, 2009.

477 Grömping, U.: Relative importance for linear regression in R: The package relaimpo, *Journal of Statistical*  
 478 *Software*, 17, 2006.

479 Hair, J. F.: *Multivariate data analysis*, 7. ed., Pearson Prentice Hall, Upper Saddle River, NJ, 785 pp., 2010.

480 Han, J., Kamber, M., and Pei, J.: *Data mining: Concepts and techniques*, 3. ed., The Morgan Kaufmann series in  
 481 data management systems, Elsevier/Morgan Kaufmann, Amsterdam, 703 pp., 2012.

482 Hartigan, J. A. and Wong, M. A.: Algorithm AS 136: A k-means clustering algorithm, *Applied Statistics*, 28,  
 483 100, doi:10.2307/2346830, 1979.

484 Hensen, B., Olsson, O., and Kümmerer, K.: A strategy for an initial assessment of the ecotoxicological effects of  
 485 transformation products of pesticides in aquatic systems following a tiered approach, *Environ. Int.*, 137,  
 486 105533, doi:10.1016/j.envint.2020.105533, 2020.

487 Imfeld, G., Meite, F., Wiegert, C., Guyot, B., Masbou, J., and Payraudeau, S.: Do rainfall characteristics affect  
 488 the export of copper, zinc and synthetic pesticides in surface runoff from headwater catchments?, *Sci. Total*  
 489 *Environ.*, 741, 140437, doi:10.1016/j.scitotenv.2020.140437, 2020.

490 Lange, J., Schuetz, T., Gregoire, C., Elsässer, D., Schulz, R., Passeport, E., and Tournebize, J.: Multi-tracer  
 491 experiments to characterise contaminant mitigation capacities for different types of artificial wetlands, *Int. J.*  
 492 *Environ. An. Ch.*, 91, 768–785, doi:10.1080/03067319.2010.525635, 2011.

493 Lefrancq, M., Imfeld, G., Payraudeau, S., and Millet, M.: Kresoxim methyl deposition, drift and runoff in a  
 494 vineyard catchment, *Sci. Total Environ.*, 442, 503–508, doi:10.1016/j.scitotenv.2012.09.082, 2013.

495 Lefrancq, M., Jadas-Hécart, A., La Jeunesse, I., Landry, D., and Payraudeau, S.: High frequency monitoring of  
 496 pesticides in runoff water to improve understanding of their transport and environmental impacts, *Sci. Total*  
 497 *Environ.*, 587-588, 75–86, doi:10.1016/j.scitotenv.2017.02.022, 2017.

498 Lewis, K. A., Tzilivakis, J., Warner, D. J., and Green, A.: An international database for pesticide risk assessments  
 499 and management, *Hum. Ecol. Risk Assess.*, 22, 1050–1064, doi:10.1080/10807039.2015.1133242, 2016.

500 Lindemann, R. H., Merenda, P. F., and Gold, R. Z.: *Introduction to bivariate and multivariate analysis*, 3rd ed.,  
 501 Scott Foresman, Glenview, 444 pp., 1980.

502 Lorenz, S., Rasmussen, J. J., Süß, A., Kalettka, T., Golla, B., Horney, P., Stähler, M., Hommel, B., and Schäfer,  
 503 R. B.: Specifics and challenges of assessing exposure and effects of pesticides in small water bodies,  
 504 *Hydrobiologia*, 793, 213–224, doi:10.1007/s10750-016-2973-6, 2017.

505 Lumley, T.: *leaps: Regression Subset Selection*, R package, 2017.

506 Maechler, M., Rousseeuw, P., Struyf, A., Hubert, M., and Hornik, K.: *cluster: Cluster Analysis Basics and*  
 507 *Extensions*. R package, 2019.

508 Maillard, E. and Imfeld, G.: Pesticide mass budget in a stormwater wetland, *Environ. Sci. Technol.*, 48, 8603–  
 509 8611, doi:10.1021/es500586x, 2014.

510 Maillard, E., Lange, J., Schreiber, S., Dollinger, J., Herbstritt, B., Millet, M., and Imfeld, G.: Dissipation of  
 511 hydrological tracers and the herbicide S-metolachlor in batch and continuous-flow wetlands, *Chemosphere*,  
 512 144, 2489–2496, doi:10.1016/j.chemosphere.2015.11.027, 2016.

513 Mersie, W., McNamee, C., Seybold, C., Wu, J., and Tierney, D.: Degradation of metolachlor in bare and  
 514 vegetated soils and in simulated water-sediment systems, *Environ. Toxicol. Chem.*, 23, 2627–2632,  
 515 doi:10.1897/04-60, 2004.

516 Moore, M. T., Rodgers Jr., J. H., Cooper, C. M., and Smith Jr., S.: Constructed wetlands for mitigation of  
 517 atrazine-associated agricultural runoff, *Environ. Pollut.*, 110, 393–399, doi:10.1016/s0269-7491(00)00034-8,  
 518 2000.

519 Oliver, D. P., Kookana, R. S., Anderson, J. S., Cox, J. W., Waller, N., and Smith, L. H.: Off-site transport of  
 520 pesticides in dissolved and particulate forms from two land uses in the Mt. Lofty Ranges, South Australia,  
 521 *Agr. Water Manage.*, 106, 78–85, doi:10.1016/j.agwat.2011.11.001, 2012.

522 Olsson, O., Khodorkovsky, M., Gassmann, M., Friedler, E., Schneider, M., and Dubowski, Y.: Fate of Pesticides  
 523 and Their Transformation Products: First Flush Effects in a Semi-Arid Catchment, *Clean (Weinh)*, 41, 134–  
 524 142, doi:10.1002/clen.201100545, 2013.

525 Passeport, E., Tournebize, J., Chaumont, C., Guenne, A., and Coquet, Y.: Pesticide contamination interception  
 526 strategy and removal efficiency in forest buffer and artificial wetland in a tile-drained agricultural watershed,  
 527 *Chemosphere*, 91, 1289–1296, doi:10.1016/j.chemosphere.2013.02.053, 2013.

528 Peter, G.: *Überfälle und Wehre: Grundlagen und Berechnungsbeispiele*, Vieweg Verlag, Wiesbaden, 320 pp.,  
 529 2005.

530 R Core Team: *R: A language and environment for statistical computing*, R Foundation for Statistical Computing,  
 531 Vienna, Austria, 2019.

532 Ramos, A., Whelan, M. J., Guymier, I., Villa, R., and Jefferson, B.: On the potential of on-line free-surface  
 533 constructed wetlands for attenuating pesticide losses from agricultural land to surface waters, *Environ.*  
 534 *Chem.*, 16, 563–576, doi:10.1071/EN19026, 2019.

535 Reichenberger, S., Bach, M., Skitschak, A., and Frede, H.-G.: Mitigation strategies to reduce pesticide inputs into  
 536 ground- and surface water and their effectiveness; a review, *Sci. Total Environ.*, 384, 1–35,  
 537 doi:10.1016/j.scitotenv.2007.04.046, 2007.

538 Schuetz, T., Gascuel-Oudoux, C., Durand, P., and Weiler, M.: Nitrate sinks and sources as controls of spatio-  
 539 temporal water quality dynamics in an agricultural headwater catchment, *Hydrol. Earth Syst. Sci.*, 20, 843–  
 540 857, doi:10.5194/hess-20-843-2016, 2016.

541 Schuetz, T., Weiler, M., and Lange, J.: Multitracer assessment of wetland succession: Effects on conservative and  
 542 nonconservative transport processes, *Water Resour. Res.*, 48, 97, doi:10.1029/2011WR011292, 2012.

543 Stang, C., Wiczorek, M. V., Noss, C., Lorke, A., Scherr, F., Goerlitz, G., and Schulz, R.: Role of submerged  
 544 vegetation in the retention processes of three plant protection products in flow-through stream mesocosms,  
 545 *Chemosphere*, 107, 13–22, doi:10.1016/j.chemosphere.2014.02.055, 2014.

546 Stehle, S., Elsaesser, D., Gregoire, C., Imfeld, G., Niehaus, E., Passeport, E., Payraudeau, S., Schäfer, R. B.,  
 547 Tournebize, J., and Schulz, R.: Pesticide risk mitigation by vegetated treatment systems: a meta-analysis, *J.*  
 548 *Environ. Qual.*, 40, 1068–1080, doi:10.2134/jeq2010.0510, 2011.

549 Taghavi, L., Merlina, G., and Probst, J.-L.: The role of storm flows in concentration of pesticides associated with  
 550 particulate and dissolved fractions as a threat to aquatic ecosystems - Case study: the agricultural watershed  
 551 of Save river (Southwest of France), *Knowl. Managt. Aquatic Ecosyst.*, 6, doi:10.1051/kmae/2011002, 2011.

552 Tournebize, J., Chaumont, C., and Mander, Ü.: Implications for constructed wetlands to mitigate nitrate and  
 553 pesticide pollution in agricultural drained watersheds, *Ecol. Eng.*, 103, 415–425,  
 554 doi:10.1016/j.ecoleng.2016.02.014, 2017.

555 Vymazal, J. and Březinová, T.: The use of constructed wetlands for removal of pesticides from agricultural runoff  
 556 and drainage: a review, *Environ. Int.*, 75, 11–20, doi:10.1016/j.envint.2014.10.026, 2015.

557 Zubrod, J. P., Bundschuh, M., Arts, G., Brühl, C. A., Imfeld, G., Knäbel, A., Payraudeau, S., Rasmussen, J. J.,  
 558 Rohr, J., Scharmüller, A., Smalling, K., Stehle, S., Schulz, R., and Schäfer, R. B.: Fungicides: An Overlooked  
 559 Pesticide Class?, *Environ. Sci. Technol.*, 53, 3347–3365, doi:10.1021/acs.est.8b04392, 2019.